Dev Genes Evol (1997) 206:464–471

ORIGINAL ARTICLE

Bernard M. Degnan · Sandie M. Degnan
Daniel E. Morse

Muscle-specific regulation of tropomyosin gene expression and myofibrillogenesis differs among muscle systems examined at metamorphosis of the gastropod *Haliotis rufescens*

Received: 17 September 1996 / Accepted: 18 December 1996

Abstract The spatial and temporal association of muscle-specific tropomyosin gene expression, and myofibril assembly and degradation during metamorphosis is analyzed in the gastropod mollusc, *Haliotis rufescens*. Metamorphosis of the planktonic larva to the benthic juvenile includes rearrangement and atrophy of specific larval muscles, and biogenesis of the new juvenile muscle system. The major muscle of the larva – the larval retractor muscle – reorganizes at metamorphosis, with two suites of cells having different fates. The ventral cells degenerate, while the dorsal cells become part of the developing juvenile mantle musculature. Prior to these changes in myofibrillar structure, tropomyosin mRNA prevalence declines until undetectable in the ventral cells, while increasing markedly in the dorsal cells. In the foot muscle and right shell muscle, tropomyosin mRNA levels remain relatively stable, even though myofibril content increases. In a population of median mesoderm cells destined to form de novo the major muscle of the juvenile and adult (the columellar muscle), tropomyosin expression is initiated at 45 h after induction of metamorphosis. Myofibrillar filamentous actin is not detected in these cells until about 7 days later. Given that patterns of tropomyosin mRNA accumulation in relation to myofibril assembly and disassembly differ significantly among the four major muscle systems examined, we suggest that different regulatory mechanisms, probably operating at both transcriptional and post-transcriptional levels, control the biogenesis and atrophy of different larval and postlarval muscles at metamorphosis.

Edited by D. Tautz

D.E. Morse
Marine Biotechnology Center and Department of Molecular, Cellular and Developmental Biology, University of California, Santa Barbara, CA 93106, USA

B.M. Degnan (✉) · S.M. Degnan
Department of Zoology and Centre for Molecular and Cellular Biology, University of Queensland, Brisbane, Qld 4072, Australia

Key words Abalone · Competence · In situ hybridization · Larva · Muscle cell

Introduction

Myogenesis and myofibrillogenesis are integrated closely in muscle cell development. Activation of the battery of muscle-specific structural genes accompanies terminal differentiation of myocytes, and represents the first step in myofibril synthesis (Epstein and Fischman 1991). We have analyzed these myogenic processes and the programmed degradation of specific muscle cells during the metamorphosis of the larva of the gastropod mollusc, *Haliotis rufescens* (red abalone). In the abalone larva, exogenous γ-aminobutyric acid (GABA; an analog of the natural GABA-mimetic peptide inducer) activates a receptor-dependent signal transduction cascade that induces the swimming larva to settle from the plankton, begin plantigrade locomotion, and metamorphose to the adult (Morse et al. 1984; Trapido-Rosenthal and Morse 1986; Baxter and Morse 1987; Morse 1992). This convenient method for the controlled, synchronous induction of metamorphosis facilitates analysis of the programmed degradation of redundant larval muscles, the rapid remodelling of larval muscles that are recruited into the emergent musculature of the juvenile, and the de novo myogenesis of juvenile muscles.

In the gastropod larva, muscle cells first develop from the mesoderm of the early trochophore (Verdonk and van den Biggelaar 1983). In *H. tuberculata*, six dorsolateral spindle-shaped muscle cells comprising the developing larval retractor muscle (LRM) elongate and migrate down the left side of the trochophore as it undergoes morphogenesis to the veliger (late larval) form. These cells converge in the posterior of the veliger, where they attach to the mantle and shell; the anterior projections of these cells diverge and attach to the velum (the larval swimming organ), mantle and foot (Crofts 1937). The numerous fibers of this LRM constitute the major muscle system of the larva. A second, smaller larval muscle –

the right shell muscle (RSM) – has been reported to give rise to the major muscle system of the adult, the columellar muscle (CM; Crofts 1937).

To characterize the morphogenesis, atrophy and restructuring of the major larval and postlarval (juvenile) muscle systems at metamorphosis in *Haliotis*, we investigated patterns of accumulation of tropomyosin mRNA and myofibrillar filamentous actin (F-actin; cf. Naganuma et al. 1994, for our related studies in tissue culture). The tropomyosin gene, encoding an actin-binding protein largely confined to the thin filaments of muscle, is regulated in a developmental stage-specific and tissue-specific manner (e.g. Karlik and Fyrberg 1986; Reinach and MacLeod 1986; MacLeod and Gooding 1988; Bandman 1992). Characterization of *Haliotis* tropomyosin mRNA accumulation in concert with analyses of the formation of myofibrillar F-actin thus allows examination of two distinct regulatory processes in the development of muscle: structural gene expression and myofibrillogenesis. Our data reveal that patterns of tropomyosin mRNA accumulation in relation to myofibril assembly and disassembly differ significantly among the four major muscle systems examined. These results indicate that different regulatory mechanisms, probably operating at both transcriptional and post-transcriptional levels, control the biogenesis and atrophy of different larval and postlarval muscles.

Materials and methods

Animals and larvae

H. rufescens adults were maintained in flowing, ambient temperature (14–16°C) sea water and induced to spawn by hydrogen-peroxide treatment (Morse et al. 1977). Larvae were maintained in the laboratory at 15°C. Nine-day-old larvae were induced to settle and metamorphose by the addition of 10^{-6} M GABA in the presence of rifampicin (2 mg/ml) as described previously (Trapido-Rosenthal and Morse 1986). A single cohort of eggs, embryos, larvae and settled juveniles was used for RNA isolation, F-actin staining and in situ hybridization analyses. Ages are indicated as hours post fertilization (hpf) and hours post induction (hpi).

BODIPY-phallacidin staining of myofibrils

Myofibrillar F-actin was stained preferentially with BODIPY-phallacidin (Molecular Probes; Burke and Alvarez 1988). Veliger larvae and plantigrade postlarvae were anesthetized by the dropwise addition of 1 M $MgCl_2$-sea water to the 100 ml cultures, and then fixed in 4% (w/v) paraformaldehyde in 100 mM Hepes (pH 6.9), 2 mM $MgSO_4$, 1 mM ethyleneglycol tetraacetic acid (EGTA) for 3 h. Fixed samples were washed twice for 5 min in phosphate-buffered saline (PBS), extracted for 1 min in cold acetone, rinsed for 30 s in PBS, incubated in a 1:10 dilution of BODIPY-phallacidin in PBS for 1 h, washed three times in PBS for 2 min each, and mounted in 1:1 PBS:glycerol. Stained samples were examined on a BioRad 600 laser confocal scanning microscope by excitation with 488-nm laser light; emission was monitored at 518 nm, and data were recorded and processed with Bio-Rad software. Optical sections from a Z-series were combined to form a partial reconstruction of larval and post-larval muscles (Matsumoto and Hale 1993) and images were photographed directly from the video screen.

Reverse transcriptase-polymerase chain reaction (RT-PCR) amplification, cloning and sequencing

cDNA templates were prepared from 168-hpf *H. rufescens* larval RNA and amplified by PCR with degenerate oligonucleotide primers that annealed to conserved regions of the tropomyosin gene – primer T1 (5′ ATGGAYGCNATHAARAARAARATGCARGCN 3′) annealed to codons 1–10, primer T2 (5′ YTCNGCNCKNGT-YTCNGCYTCYTTNARYTT 3′) to codons 240–231. The resultant RT-PCR product was blunt-ended, gel purified and cloned into pBSK+ (Stratagene), and six randomly selected recombinant colonies were sequenced. Methods for preparation of total RNA and cDNA, PCR amplification, cloning and sequencing were as described in Degnan and Morse (1993).

Tropomyosin gene-specific primers were used for the amplification of 5′ and 3′ cDNA ends (RACE; Frohman et al. 1988); TGS1 (5′ CTTCTGCTCTTCGGTATCCCTT 3′) annealed to codons 36–30, and TGS2 (5′ CAGTGAACAAGAGGCATCTCAG 3′) to codons 209–216. For 5′ RACE, cDNA was tailed in the presence of terminal transferase and dCTP using a 5′ RACE kit (BRL). The 5′ RACE product was generated by amplifying this tailed cDNA using an anchor primer (5′ GGCCACGCGTCGA-CTAGTACGGGIIGGGIIGGGIIG 3′) and TGS1 following the instructions of the manufacturer. For 3′ RACE, oligo(dT) adaptor-primed (5′ GGCCACGCGTCGACTAGTAC$(T)_{17}$ 3′) cDNA was amplified using an adaptor primer (5′ GGCCACGCGTCGACT-AGTAC 3′) and TGS2 following the instructions of the manufacturer. The major 5′ and 3′ RACE products were purified, cloned and three randomly selected recombinant colonies sequenced. The 5′ RACE clones were cycle sequenced using TGS1, and either SK or KS primers. The 3′ RACE clones were sequenced with TGS2, SK or KS, and two tropomyosin-specific sense primers that annealed to the 3′ untranslated region.

Northern and in situ hybridization analyses

For northern hybridization analyses, 7.5 μg of total RNA/lane was resolved on a 1% agarose/formaldehyde denaturing gel and capillary blotted onto Hybond-N membrane (Amersham). Probes were synthesized from a linearized recombinant plasmid containing the PCR product corresponding to codons 1–240 of the open reading frame (ORF) (pTR1A), using T3 and T7 RNA polymerases in a reaction mixture containing digoxigenin-11 uridine triphosphate (UTP). The membrane was hybridized with the antisense digoxigenin-labeled tropomyosin riboprobe, under stringent conditions, following the protocol recommended by the manufacturer of the digoxigenin-11-UTP (Boehringer-Mannheim); after hybridization the membrane was washed three times in 0.5 × sodium sodium citrate (SSC), 0.1% sodium dodecyl sulfate (SDS) at 65°C. An autoradiograph detecting the hybridization signal was obtained by reaction with an alkaline phosphatase-conjugated anti-digoxigenin antibody, wetting the membrane with fluorogenic substrate (Lumiphos 530; Boehringer-Mannheim) and exposure to XAR film (Kodak) for 5 min.

Whole mount in situ hybridizations were performed as described in Degnan et al. (1995). Specifically, *Haliotis* larvae and postlarvae were hybridized to digoxigenin-labeled anti-sense and sense tropomyosin cDNA riboprobes at 0.1 ng probe/μl hybridization solution. Prior to use, riboprobes were hydrolyzed in 30 mM Na_2CO_3, 20 mM $NaHCO_3$ (pH 10.2) at 60°C for 10 min, and neutralized by the addition of an equal volume of 200 mM NaOAc, 1% (v/v) acetic acid (pH 6.0; Cox et al. 1984). The sense riboprobe was used as a negative control in the hybridization analyses. Hybridization patterns were visualized by light microscopy using a Zeiss microscope equipped with Normarski optics.

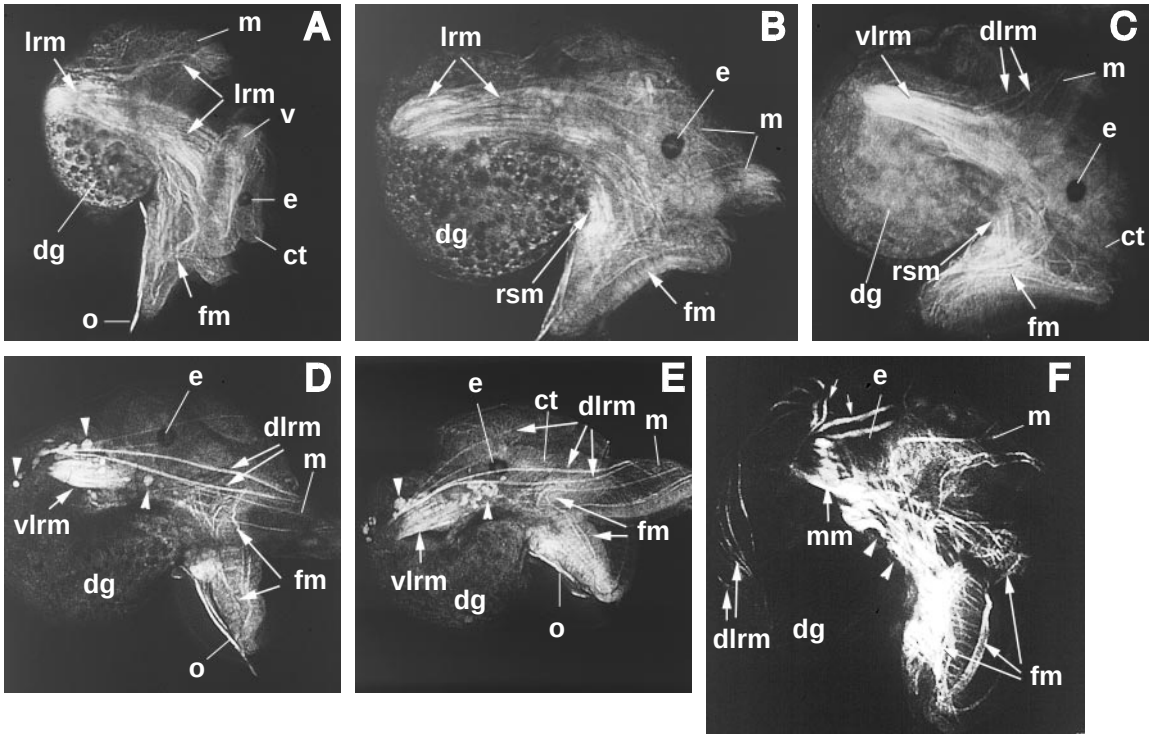

Fig. 1A–F Changes in distribution of BODIPY-phallacidin-labeled myofibrillar F-actin during metamorphosis. All confocal micrographs are lateral views with anterior to *right*. **A** Veliger larva of 168 hours post fertilization (hpf) with fully developed larval musculature; the larval retractor muscle (LRM; *lrm*), originating posteriorly, has extensive connections to head, foot, velum and mantle; the foot musculature (*fm*) is well developed and individual myofibers are present in the head and cephalic tentacle. **B** Postlarva of 24 hours post induction (hpi); LRM myofibril staining is reduced in cephalopedal region; myofibrils associated with mantle remain intact; the right shell muscle (RSM; *rsm*) is stained intensely. **C** Postlarva of 42 hpi; myofibrils of LRM increase in prominence in posterior portion of ventral fibers (*vlrm*) and remain intact throughout dorsal LRM (*dlrm*); myofibril content of foot and RSM have increased. **D** Postlarva of 70 hpi; numerous fluorescent cell bodies (*arrowheads*) and shortened myofibrils are all that remain in posterior region of ventral LRM; dorsal LRM in the mantle are evident; foot musculature continues to increase. **E** Postlarva of 96 hpi; mantle and foot myofibrillar content increase; fluorescent cell bodies (*arrowheads*) and shortened ventral LRM myofibrils are still present. **F** Postlarva of 204 hpi; dramatic increases in myofibrillar content of posterior portion of foot and median mesoderm cells (*mm*); new myofibrils connect these two regions (*arrowheads*); myofibrils also project from mesoderm to head and mantle (*small arrows*). Increased myofibril content and phallacidin staining reduce relative contribution of background autofluorescence; LRM-derived mantle myofibrils (*dlrm*) are faint relative to foot and new myofibrils. Larva and postlarvae are 200 μm maximum diameter in all panels (magnifications differ). (*ct* cephalic tentacle, *dg* digestive gland, *e* eye spot, *m* mantle, *o* operculum, *v* velum)

Results

Myofibrillogenesis and muscle atrophy at metamorphosis

Myofibrillar F-actin was detected by laser confocal microscopy after BODIPY-phallacidin staining. In this section, we describe myofibrillar structure and amount in each of four muscle systems (the larval retractor muscle, the right shell muscle, the foot muscle and the columellar muscle), first at a representative stage prior to induction of metamorphosis and then in a time series post-induction.

At 168 hpf, the veliger larvae became competent to settle and metamorphose (Morse 1992). At this stage, the LRM projected from the posterior shell attachment plaque to the mantle and cephalopedal regions (Fig. 1A). The RSM and extensive foot musculature was present, and an extensive network of single, discrete myofibrils was located under the epidermis throughout the velum and cephalopedal region, including the cephalic tentacles (Fig. 1A). No further increase in muscle size or complexity in any of the muscles was observed after this stage until metamorphosis was induced.

Within 24 h post-GABA induction (hpi), plantigrade attachment, abscission of the larval velum and initiation of adult shell synthesis occurred. At this time, increased BODIPY-phallacidin staining of the posterior terminus of the LRM was observed (Fig. 1B). This apparently was the result of the severance of the anterior LRM connections to the velum, and the consequent posterior contraction of the fibers of this larval muscle. Some LRM attachments to the foot remained intact until after 42 hpi (Fig. 1C). By 70 hpi, the LRM had lost all connection with the cephalopedal region and the ventral LRM cells had degenerated to short myofibrillar assemblies or disorganized F-actin-containing cell bodies (Fig. 1D). There was no significant change in myofibril staining in these ventral cells from 70 to 134 hpi (Fig. 1D, E and data not shown). In marked contrast, there was a conspicuous increase of myofibrillar content of the dorsal LRM cells during this period. After 134 hpi, only the dorsal LRM was detectable by phallacidin staining (not shown).

In the foot, myofibrillar content was observed to increase slightly following the induction of metamorphosis. Between 42 and 204 hpi, the musculature of the posterior region of the foot increased significantly (Fig. 1C–F), with two primary bands of this new muscle encircling the dorsal and ventral edges of the foot, connected by a row of evenly spaced secondary fibers (Fig. 1D–F). The RSM showed no detectable change in size following induction of metamorphosis.

In the median mesoderm of the post-larva, there was a first appearance of myofibrillar F-actin at 204 hpi (Fig. 1F); F-actin was not detected in this region at 188 hpi (not shown). The new myofibrils projected dorsoventrally from the posterior of the foot to the cephalic region between the eyes (Fig. 1F). These large F-actin-containing mesodermal cells were located in the region of the CM, the major muscle system of the adult.

Tropomyosin sequence analysis

Sequence analysis of clones derived from the degenerate oligonucleotide RT-PCR, and 5′ and 3′ RACE products (720, 366 and 1406 bp, respectively) confirmed that all of the PCR products analyzed represented the same tropomyosin sequence. A composite 2217-bp *H. rufescens* tropomyosin (*HrTM1*) cDNA sequence was obtained (GenBank/EBI accession No. X75218). The deduced *HrTM1* protein sequence conformed closely to the structure of other metazoan tropomyosins, exhibiting a periodic distribution of hydrophobic and charged residues in a contiguously repetitive peptide of 7 residues (McLachlan et al. 1975). Of the 82 residues, 73 at the 1st and 4th positions of this canonical repeating heptapeptide in *HrTM1* are hydrophobic, and 56 of the 80 residues at the 5th and 7th positions are charged; the properties of the residues at these positions form the basis of the coiled-coil structure of tropomyosin (McLachlan et al. 1975; Karlik and Fyrberg 1986; Mische et al. 1987). The deduced sequence of HrTM1 exhibits varying degrees of similarity to the tropomyosins of other metazoans (Fig. 2), being most similar to tropomyosins expressed in the gastropod mollusc *Biomphalaria glabrata* (80–84.2% identity), and the trematode flatworm *Schistosoma mansoni* (62.6–67.7% identity; Xu et al. 1989; Dissous et al. 1990; Weston and Kemp 1993); *HrTM1* is less similar to the *Drosophila* tropomyosins (51.8–56.6%; Basi and Storti 1986; Karlik and Fyrberg 1986). Being expressed in larval and postlarval muscle, *HrTM1* is more similar to vertebrate skeletal and cardiac muscle (50.9–53.9%) tropomyosins than smooth muscle tropomyosins (48.9–49.6%; MacLeod et al. 1985; Mische et al. 1987; Lin and Leavitt 1988; MacLeod and Gooding 1988; Widada et al. 1988; Fig. 2).

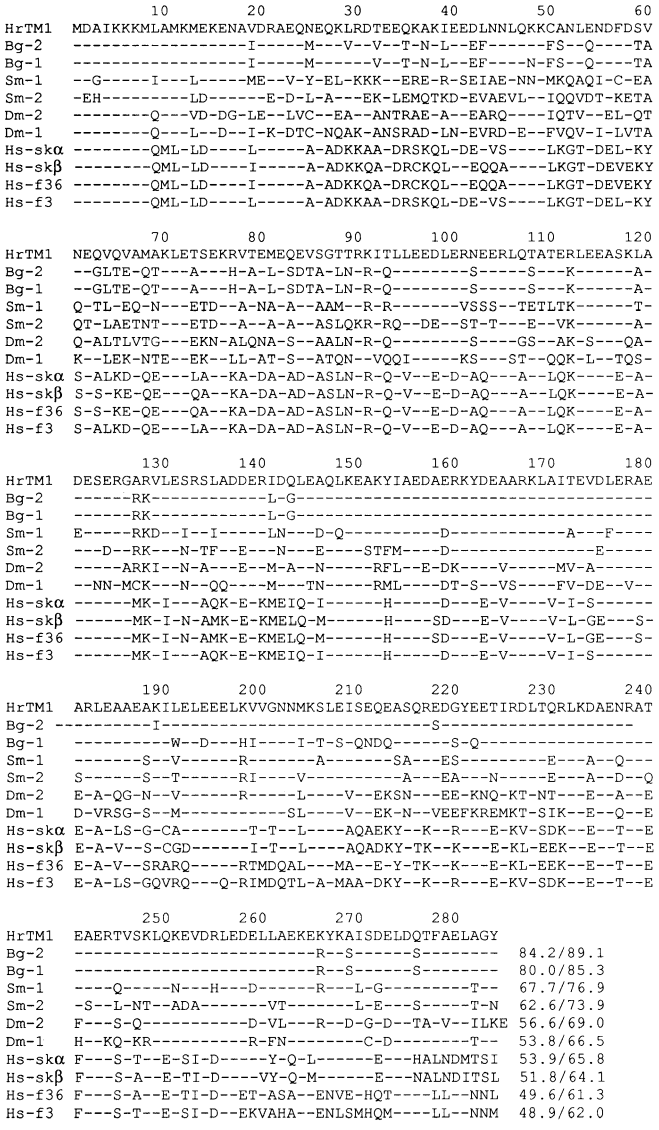

Fig. 2 Alignment of derived tropomyosin protein sequence from *Haliotis rufescens* (*HrTM1*) with muscle tropomyosin isoforms from the gastropod *Biomphalaria glabrata* (*Bg*), the trematode *Schistosoma mansoni* (*Sm*; Xu et al. 1989; Dissous et al. 1990; Weston and Kemp 1993), *Drosophila* (*Dm*; Basi and Storti 1986; Karlik and Fyrberg 1986), and human (*Hs*) skeletal muscle (*sk*; Mische et al. 1987; MacLeod and Gooding 1988; Widada et al. 1988) and fibroblasts (*f*; MacLeod et al. 1985; Lin and Leavitt 1988). *Dashes* indicate identity; *paired values* at the end of each sequence indicate percent of identity with *Haliotis* sequence and percent identity including conservative substitutions (I/V/L; T/S; R/K; D/E; N/Q; F/Y/W)

Developmental appearance of the 2.3 knt *HrTM1* mRNA

Northern blot analysis of total RNA from egg, embryos, larvae and postlarvae demonstrated that a single tropomyosin transcript of approximately 2.3 knt hybridized to the cloned 720-bp PCR product, and accumulated through larval and early post-metamorphic development (Fig. 3). The *HrTM1* probe used in this investigation corresponds to conserved codons 1–240, and should cross-hybridize with transcripts encoding other tropomyosin isoforms expressed from the same locus (cf. Karlik and Fyrberg 1986), but not necessarily those from other loci (e.g. Bautch et al. 1982). This *HrTM1* mRNA was first

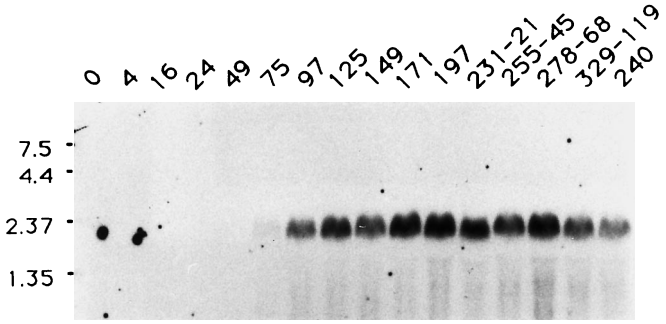

Fig. 3 Northern blot analysis of *HrTM1* transcript accumulation through embryogenesis, larval development and metamorphosis. Competent larvae were induced to settle and begin metamorphosis at 210 hpf. Each lane contained 7.5 µg total RNA. The rRNA bands in each lane were of equal intensity in the ethidium bromide-stained gel and on the membrane after transfer (not shown), indicating equal loading of RNA. *Numbers in horizontal row* are hours post fertilization (hpf), followed where appropriate by hpi (for samples from induced postlarvae); *numbers at left* are knt from standard. 0 hpf = unfertilized eggs; 4 hpf = 16-cell embryos; 16 hpf = late gastrulae; 24 hpf = hatched trochophore larvae; 24–75 hpf = developing larvae; 97–149 hpf = veliger larvae, 171–240 hpf = veliger larvae competent to metamorphose; 21–119 hpi = postlarvae undergoing metamorphosis

detected in the 24-hpf larvae (upon longer exposure of the northern blot hybridization filter in Fig. 3) and continued to accumulate to about 171 hpf; this is close to the time at which the veliger larva becomes competent to settle and metamorphose (Morse 1992). There were small changes in the level of *HrTM1* abundance during early metamorphosis, with overall transcript abundance decreasing by 119 hpi (equivalent to 329 hpf). In sibling larvae that were not induced to metamorphose, transcript abundance decreased earlier, by 240 hpf (Fig. 3, last lane).

Spatial expression of *HrTM1* during metamorphosis

HrTM1 expression was detected by light microscopy after whole-mount in situ hybridization using digoxigenin-labeled cDNA riboprobes. In this section, we describe patterns of *HrTM1* expression in each of four major muscle systems (the LRM, RSM, foot muscle and CM), first at a representative stage prior to induction of metamorphosis and then in a time series post induction.

In the 168-hpf competent veliger larva, *HrTM1* mRNA was detected in the LRM, RSM, mantle, foot, head and cephalic tentacles (Fig. 4A), in a spatial pattern which resembled that of myofibrillar F-actin staining

Fig. 4A–F Spatial accumulation of *HrTM1* mRNA during metamorphosis. All micrographs are lateral views with anterior *to right*, except D which is a dorsal view with anterior *to lower right corner*. Abbreviations as in Fig. 1. **A** Veliger larva of 168 hpf; *HrTM1* transcripts present in LRM, RSM, foot (*f*), mantle and cephalic tentacle muscles. **B** Postlarva of 24 hpi; *HrTM1* mRNA abundant in most dorsal LRM cells; transcripts rare in ventral LRM cells. **C**, **D** Postlarvae of 45 hpi; transcripts limited to mantle LRM cells (*dlrm*), foot and a population of dorsal median mesoderm cells (*cmp* CM progenitors); dorsal view (**D**) shows that the distribution of cmp cells expressing tropomyosin is bilaterally symmetrical; no transcripts detectable in ventral LRM. **E** Postlarva of 94 hpi; transcripts abundant in foot, RSM and CM progenitors. **F** Postlarva of 188 hpi; transcripts remain abundant in foot, RSM and CM progenitors. Larva and postlarvae are 200 µm maximum diameter

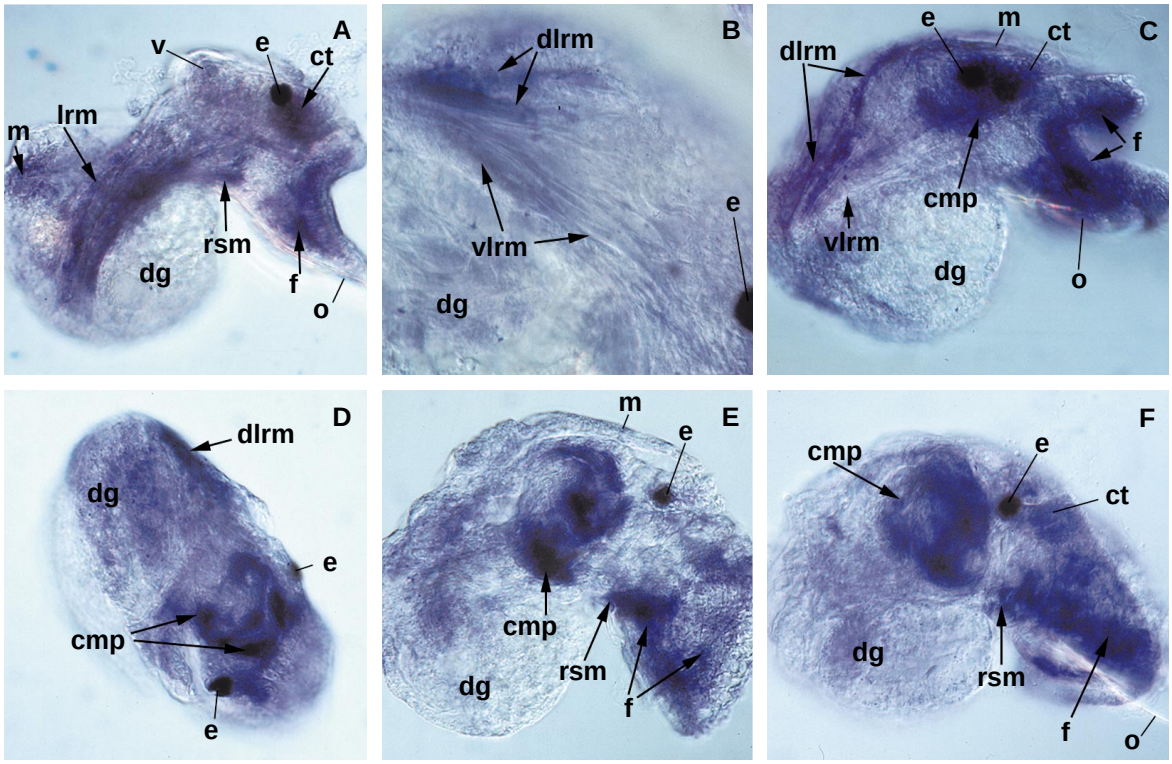

(Fig. 1A). In both the foot and RSM, the amount and distribution of *HrTM1* mRNA remained stable from this stage right through to 188 hpi (Fig. 4).

At 24 hpi, *HrTM1* mRNA was detected primarily in the posterior ends of the most dorsal cells of the LRM (Fig. 4B), the most dorsal cells being those which remain associated with the mantle of the postlarva. By 45 hpi, transcripts were detected along the entire length of these dorsal LRM cells (Fig. 4C), but this expression subsequently decreased from about 94 hpi onwards (Fig. 4E, F) despite the presence of myofibrillar F-actin in these cells at this stage (Fig. 1E, F). A contrasting pattern was observed in the ventral cells of the LRM, which attach anteriorly to the velum and the cephalopedal domain. Here, *HrTM1* expression decreased substantially between the veliger stage at 168 hpf and the postlarva at 24 hpi (Fig. 4A, B), and transcripts were no longer detectable by 45 hpi (Fig. 4C).

In a discrete population of cells in the median mesoderm located behind the eyes, there was a sudden and dramatic accumulation of *HrTM1* transcripts at 45 hpi (Fig. 4C, D), followed by progressively more ventral mesodermal expression from 94 to 188 hpi (Fig. 4E, F). This expression corresponds to a region of F-actin accumulation in the 204-hpi postlarva (Fig. 1F). In this context, it is of interest that Crofts (1937) reported from light microscopy studies on *H. tuberculata* that the CM, the major muscle of the adult, appeared to arise from the RSM. Our observations of *HrTM1* mRNA accumulation (Fig. 4) and myofibrillar staining (Fig. 1) in *H. rufescens* suggest instead that the CM develops from these myogenic cells in the dorsomedial mesoderm, which subsequently extend both ventrally and dorsally to connect the foot to the dorsal shell.

Discussion

The in situ hybridization analyses described here have revealed complex spatial and temporal changes in *HrTM1* mRNA accumulation in *H. rufescens* muscles during metamorphosis. One interpretation of this complexity could be that divergent tropomyosin transcripts are being expressed simultaneously in larval and postlarval muscles. Indeed, there are cases in other (non-molluscan) animals where different isoforms of muscle tropomyosin mRNA, derived from a single locus, each are expressed in a developmentally-restricted manner (Karlik and Fryberg 1986; MacLeod and Gooding 1988). However, these cases were easily detectable via northern blot analyses conducted with a single tropomyosin probe, because the different isoforms typically are encoded by transcripts of different lengths. In molluscs, electrophoretic analyses of adult muscle tropomyosin have lead to the general conclusion that only a single peptide exists, in contrast to the two chains found in vertebrates (reviewed in Chantler 1983), although more sophisticated analyses recently have revealed two tropomyosin cDNAs, with open reading frames (ORFs) of 94.7% identity, in the gastropod *B. glabrata* (Dissous et al. 1990; Weston and Kemp 1993). Using degenerate primers T1 and T2, and the RT-PCR and cloning procedures described above, we recently identified a single tropomyosin gene that is expressed in the adult columellar and mantle muscles of the tropical abalone, *H. asinina* (Counihan and Degnan, unpublished data) and is nearly identical to *HrTM1* (the first 917 nt, comprising the 5′ UTR and a portion of the ORF, are 94.9% identical and the first 230 amino acids are 96.5% identical). The identification of a very similar tropomyosin gene in a different species of *Haliotis* supports the contention that a single tropomyosin is expressed in the major muscles of the abalone larva, postlarva and adult.

As evidence against the ‘multiple-transcript’ interpretation in our case, we point out that (i) northern blot analysis indicated that only one size of tropomyosin transcript hybridized to the probe (corresponding to residues 1–240 of the ORF) used in this study, (ii) PCR amplification with degenerate oligonucleotide primers generated only a single tropomyosin product, and (iii) identical in situ hybridization results were obtained using a 3′ riboprobe corresponding to nts 869–2217 (results not shown). We acknowledge that these experimental results cannot preclude completely the possibility that multiple types of tropomyosin mRNA are simultaneously expressed in the developing *Haliotis* larvae or postlarvae. However, comparison of the in situ hybridization data with those on the accumulation of myofibrillar F-actin strongly suggests that the 2.3 knt *HrTM1* mRNA is expressed in most, if not all, larval and postlarval muscles.

Changes in *HrTM1* mRNA in LRM cells at metamorphosis

The induction of separate fates of the dorsal and ventral cells of the LRM at metamorphosis is documented both by the changes in LRM myofibrillar structure (Fig. 1) and by the differential accumulation of *HrTM1* mRNA (Fig. 4). Crofts (1937) long ago observed via light microscopy that, at metamorphosis in *H. tuberculata*, some of the LRM cells atrophy, while others become incorporated into the developing musculature of the adult mantle. We did not determine if the ventral LRM cells exhibit all of the characteristics of apoptosis (cf. Coles et al. 1993), but we would argue that the (i) disassembly of the myofibrillar apparatus, (ii) shrinkage and apparent fragmentation of these muscle cells (resulting in the observed increase in the number of ventral F-actin-staining bodies during metamorphosis), and (iii) subsequent disappearance of these F-actin-staining bodies together suggest that these ventral LRM cells undergo a form of programmed atrophy, as predicted by Crofts (1937).

Within 24 h of the induction of metamorphosis, we observed a differential response in the ventral and dorsal cells of the LRM; *HrTM1* mRNA decreased to undetectable in the ventral cells, while increasing markedly in the dorsal cells (Fig. 4B, C). The depletion of transcripts in

the ventral LRM occurred approximately 48 h before gross myofibrillar degeneration (Figs. 1, 4), suggesting that a programmed pathway specifying the destruction of certain myofibrils is regulated by morphogenetic signals that originate from the larval chemosensory receptors (cf. Degnan and Morse 1995). Programmed cell death is a common fate of redundant larval tissues at metamorphosis in a wide range of taxa (Ellis et al. 1991). In the moth, *Manduca sexta*, the intersegmental muscle cells die during metamorphosis; prior to death, the number of actin and myosin mRNAs and proteins in these cells is reduced by repression of gene expression (Schwartz et al. 1993). Our data from *H. rufescens* suggest that either repression of *HrTM1* (cf. Schwartz et al. 1993) and/or increased mRNA degradation is occurring in the ventral cells of the LRM. In contrast, in the dorsal cells of the LRM, *HrTM1* mRNA increased before we saw the changes in myofibril content that correspond to a transition from larval to adult muscle form (Figs. 1, 4). Our data thus indicate that induction or repression of *HrTM1* mRNA accumulation occur differentially in the two discrete populations of cells in the LRM prior to changes in the muscle phenotype. These simultaneous and opposite responses to morphogenic activation suggest that either preexisting differences in these cells, or a signaling event along the dorsoventral axis, might be responsible for the differential specification of dorsal and ventral LRM cell fates.

Accumulation of *HrTM1* mRNA precedes myofibrillogenesis in the columellar muscles

In the postlarval CM, there is a significant lag between *HrTM1* mRNA accumulation and myofibril assembly. At metamorphosis, *HrTM1* transcript accumulation in the median mesoderm begins almost 7 days prior to myofibrillar assembly (Figs. 1, 4). This is in contrast to the LRM, RSM and foot musculature, in all of which myofibrillar assembly appears to be more closely coupled temporally with *HrTM1* mRNA accumulation. These results suggest that different post-transcriptional regulatory mechanisms may be operating to control myofibrillogenesis in different populations of myoblasts. For example, it is possible that, in the *Haliotis* CM, other essential myofibrillar gene products are not synthesized concomitantly with HrTM1, thus preventing myofibril assembly in concert with the accumulation of *HrTM1* mRNA. A majority of vertebrate sarcomeric structural gene mRNAs accumulate within 1 day of maturation of muscle fibers (e.g. Cox et al. 1991; Lyons et al. 1991), but there are cases of greater time lags in other gene systems. For example, perinatal myosin heavy chain (MHC) mRNA accumulates in mouse myogenic cells 5.5 days prior to perinatal MHC detection (Lyons et al. 1990). With this mouse example in mind, we argue that our results are consistent with the suggestion that translational and/or post-translational regulatory mechanisms can control myofibril assembly. The dramatic onset of myofibrillogenesis in CM progenitors (Fig. 1F) suggests that the prior accumulation of large quantities of structural gene mRNA may be part of a developmental mechanism to facilitate rapid myogenesis and muscle growth in this tissue. Complete elucidation of the regulatory mechanisms governing myofibril assembly will require characterization of transcript accumulation for the other structural genes involved, and analyses of translation and degradation of the messenger transcripts.

Acknowledgements We thank N. Hooker and J. Hydanus for their expert assistance in the production and cultivation of the larvae, and R. Counihan for the use of unpublished sequence data. This research was supported by grants to D.E.M. from the National Institutes of Health (#R01-RR06640 and #R01-CA53105) and the NOAA National Sea Grant College Program, Department of Commerce, under grant NA36RG0537, Project R/A-91 through the California Sea Grant College Program and the California State Resources Agency, and to B.M.D. from the Australian Research Council. The U.S. Government is authorized to reproduce and distribute the findings for governmental purposes.

References

Bandman E (1992) Contractile protein isoforms in muscle development. Dev Biol 154: 273–283

Basi GS, Storti RV (1986) Structure and DNA sequence of the tropomyosin I gene from *Drosophila melanogaster*. J Biol Chem 261: 817–827

Bautch VL, Storti RV, Mischke D, Pardue ML (1982) Organization and expression of *Drosophila* tropomyosin genes. J Mol Biol 162: 231–250

Baxter G, Morse DE (1987) G protein and diacylglycerol regulate metamorphosis of planktonic molluscan larvae. Proc Natl Acad Sci USA 84: 1867–1870

Burke RD, Alvarez CM (1988) Development of the esophageal muscles in embryos of the sea urchin *Strongylocentrotus purpuratus*. Cell Tissue Res 252: 411–417

Chantler PD (1983) Biochemical and structural aspects of molluscan muscle. In: Saleuddin ASM, Wilbur KM (eds) The Mollusca, vol 4. Academic Press, New York, pp 77–154

Coles HSR, Burne JF, Raff MC (1993) Large-scale normal cell death in the developing rat kidney and its reduction by epidemal growth factor. Development 118: 777–784

Cox KH, DeLeon DV, Angerer LM, Angerer RC (1984) Detection in sea urchin embryos by in situ hybridization using asymmetric RNA probes. Dev Biol 101: 485–502

Cox RD, Weydert A, Barlow D, Buckingham ME (1991) Three linked myosin heavy chain genes clustered within 370 kb of each other show independent transcriptional and post-transcriptional regulation during differentiation of the mouse muscle cell line. Dev Biol 143: 36–43

Crofts DR (1937) The development of *Haliotis tuberculata*, with special reference to organogenesis during torsion. Phil Trans R Soc London 228B: 219–268

Degnan BM, Morse DE (1993) Identification of eight homeobox-containing transcripts expressed during larval development and at metamorphosis in the gastropod mollusc *Haliotis rufescens*. Mol Mar Biol Biotech 2: 1–9

Degnan BM, Morse DE (1995) Developmental and morphogenetic gene regulation in *Haliotis rufescens* larvae at metamorphosis. Am Zool 35: 391–398

Degnan BM, Groppe JC, Morse DE (1995) Chymotrypsin mRNA expression in digestive gland amoebocytes: cell specification occurs prior to metamorphosis and gut morphogenesis in the gastropod *Haliotis rufescens*. Roux's Arch Dev Biol 205: 97–101

Dissous C, Torpier G, Duvaux-Miret O, Capron A (1990) Structural homology of tropomyosins from the human trematode

Schistosoma mansoni and its intermediate host *Biomphalaria glabarata*. Mol Biochem Parasitol 43: 245–256
Ellis RA, Yuan J, Horvitz HR (1991) Mechanisms of cell death. Annu Rev Cell Biol 7: 663–698
Epstein HF, Fischman DA (1991) Molecular analysis of protein assembly in muscle development. Science 251: 1039–1044
Frohman MA, Dush MK, Martin GR (1988) Rapid production of full length cDNAs from rare transcripts: Amplification using a single gene-specific oligonucleotide primer. Proc Natl Acad Sci USA 85: 8998–9002
Karlik CC, Fyrberg EA (1986) Two *Drosophila melanogaster* tropomyosin genes: structural and functional aspects. Mol Cell Biol 6: 1965–1973
Lin CS, Leavitt J (1988) Cloning and characterization of a cDNA encoding transformation-sensitive tropomyosin isoform 3 from tumorigenic human fibroblasts. Mol Cell Biol 8: 160–168
Lyons GE, Ontell M, Cox R, Sassoon D, Buckingham ME (1990) The expression of myosin genes in developing skeletal muscle in the mouse embryo. J Cell Biol 111: 1465–1476
Lyons GE, Buckingham ME, Mannherz HG (1991) α-actin proteins and gene transcripts are colocalized in embryonic mouse muscle. Development 111: 451–454
MacLeod AR, Gooding C (1988) Human hTMα gene: expression in muscle and nonmuscle tissue. Mol Cell Biol 8: 433–440
MacLeod AR, Houlker C, Reinach FC, Smillie LB, Talbot K, Modi G, Walsh FS (1985) A muscle-type tropomyosin in human fibroblasts: evidence for expression by an alternative RNA splicing mechanism. Proc Natl Acad Sci USA 82: 7835–7839
Matsumoto B, Hale IL (1993) Preparation of retinas for studying photoreceptors with confocal microscopy. In: Hargrave P (ed) Methods in neurosciences, vol 15. Academic Press, San Diego, pp 54–71
McLachlan AD, Stewart M, Smillie LB (1975) Sequence repeats in an a tropomyosin. J Mol Biol 98: 281–291
Mische SM, Manjula BN, Fischetti VA (1987) Relation of streptococcal M protein with human and rabbit tropomyosin: the complete amino acid sequence of human and cardiac alpha tropomyosin, a highly conserved contractile protein. Biochem Biophys Res Commun 142: 813–818
Morse ANC, Froyd C, Morse DE (1984) Molecules from cyanobacteria and red algae that induce larval settlement and metamorphosis in the mollusc *Haliotis rufescens*. Mar Biol 81: 293–298
Morse DE (1992) Molecular mechanisms controlling metamorphosis and recruitment in abalone larvae. In: Shepherd SA, Tegner MJ, Guzman del Proo SA (eds) Abalone of the world: Ecology, fisheries and culture. Blackwell, Oxford, pp 107–119
Morse DE, Duncan H, Hooker N, Morse A (1977) Hydrogen peroxide induces spawning in molluscs, with activation of prostaglandin endoperoxide synthetase. Science 196: 298–300
Naganuma T, Degnan BM, Horikoshi K, Morse DE (1994) Myogenesis in primary cell cultures from larvae of the abalone, *Haliotis rufescens*. Mol Mar Biol Biotechnol 3: 131–140
Reinach FC, MacLeod AR (1986) Tissue-specific expression of the human tropomyosin gene involved in the generation of the *trk* oncogene. Nature 322: 648–650
Schwartz LM, Jones MEE, Kosz L, Kuah K (1993) Selective repression of actin and myosin heavy chain expression during programmed death of insect skeletal muscle. Dev Biol 158: 448–455
Trapido-Rosenthal HG, Morse DE (1986) Availability of chemosensory receptors is down regulated by habituation of larvae to a morphometric signal. Proc Natl Acad Sci USA 83: 7658–7662
Verdonk NH, Biggelaar JAM van den (1983) Early development and the formation of germ band layers. In: Verdonk NH, Biggelaar JAM van den, Tompa AS (eds) The Mollusca, vol 3. Academic Press, New York, pp 91–122
Weston DS, Kemp WM (1993) *Schistosoma mansoni*: Comparison of cloned tropomyosin antigens shared between adult parasites and *Biomphalaria glabrata*. Exp Parasitol 76: 358–370
Widada JS, Ferraz C, Capony JP, Liautard JP (1988) Complete nucleotide sequence of the adult skeletal isoform of human skeletal muscle β-tropomyosin. Nucleic Acids Res 16: 3109
Xu H, Miller S, van Keulen H, Wawrzynski MR, Rekosh DM, LoVerde PT (1989) *Schistosoma mansoni* tropomyosin: cDNA characterization, sequence, expression and gene product localization. Exp Parasitol 69: 373–392